

Modified Michelson Interferometer Design for Ear Measurement

Raya Badie Younis¹, Suha Mousa Khorsheed², Ziad Tarik Al-Dahan³

¹Al-Nahrain University/College of Engineering/ Biomedical Engineering Department, Baghdad, Iraq

²Al-Nahrain University/College of Science/Physics Department, Baghdad, Iraq

³Al-Nahrain University/College of Engineering/ Biomedical Engineering Department, Baghdad, Iraq

Abstract: This paper presents an experimental study of the laser interferometry technique. Zemax OpticStudio was employed to model Michelson interferometer for eardrum evaluation. Zemax Optical Design simulation was performed to specify the proper dimensions of Michelson interferometer for achieving best performance. A default configuration of Michelson interferometer was modeled, in terms of variant scaled configuration to reduce the dimensions and improve the resolution. Therefore, simulated eardrum characteristics were evaluated in response to pure tone sound stimulations. The measurement results show that the proposed design was able to detect nanometer displacement of the tympanic membrane with a high sensitivity.

Keywords: laser Doppler interferometer, Michelson, OpticStudio, Zemax, optical interferometer

1. Introduction

Optical interferometer is a powerful tool that allows noncontact optical analysis of small vibrations objects with high accuracy by means of Doppler effect. The idea is to use an optical interferometer for measuring the frequency shift of a laser beam that is reflected back from the vibrating object. The reflected beam interferes with the reference beam to produce an optical signal whose beat frequency is equal to that of the difference between the two beams. Such that, the displacement of the object can be precisely measured [1]. Many types of interferometers can be used in such technique, but they differ in their configuration. Michelson interferometer is simple and most widely known type. In which, the light beam from a coherent source will be divided by a beam splitter, the first beam is reflected by a reference surface and the other is reflected by a test surface as shown in Fig 1. Each of these beams travels in a different path, the difference in the distance traveled by each beam, creates a phase difference between them and leads to make the interference pattern [2].

Biologically, the human ear is divided into three parts: the outer ear, the middle ear, and the inner ear as illustrated in Fig 2. The auricle funnels sound waves extended from the outside to the external auditory canal and from there to the middle ear. The middle ear consists of an air-filled cavity, a tympanic membrane, and the ossicles bones (malleus, incus and stapes) suspended in the middle ear cavity by suspensory ligaments. These together constitute a mechanical system responsible for sound transmission from the external ear canal to the inner ear [4]. In medicine, optical interferometer provides unique accurate tool for precision vibrations measurements [3]. One of the most important medical applications is the measurement of tympanic membrane vibrations pattern that stimulated by sound. Tympanic membrane displacement measurement allows accurate detection of various middle ear disorders.

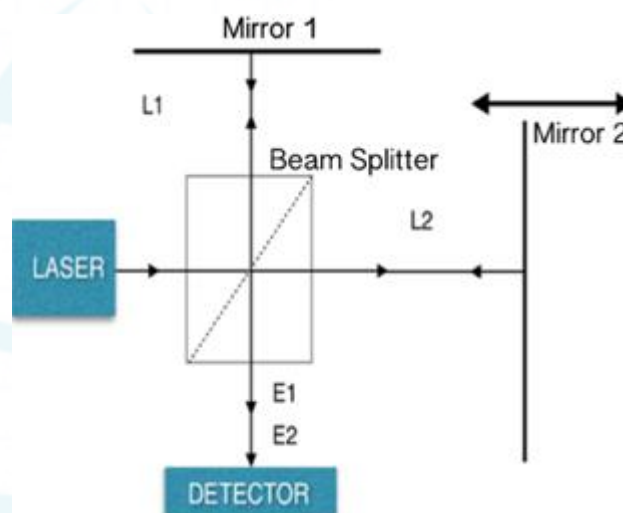


Figure 1: Simplified scheme of Michelson

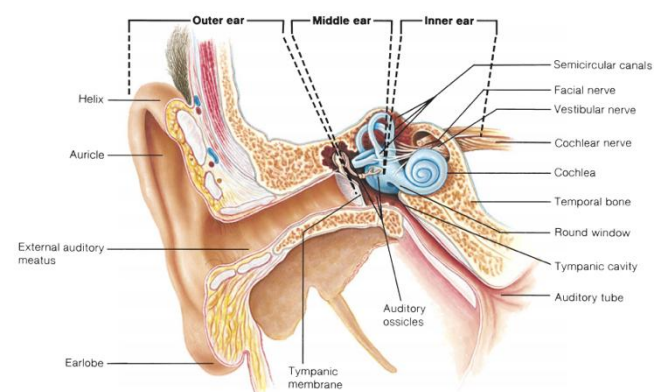


Figure 2: External, middle, and internal portions of the right ear [5]

2. Related Work and Contribution

The eardrum vibrations measurement has attracted a lot of research. The applications field was still searching for an accurate method that can be used to improve the simulated

results. The most interested researches besides our contribution are briefly explained in the following subsections.

3. Related Work

There are many papers were devoted to eardrum vibration measurement. They are different in many aspects such as; used measurement design, adopted approach, or even the limitations of application. In the following, we focus on some researches that dealing with the considered problem of enhancing wave detection details for purpose of eardrum vibration simulation in different application field:

The feasibility of using laser Doppler interferometer (LDI) for a preoperative differential diagnosis of a conductive hearing loss was investigated in [6], then compared it with standard audiometry, both of their results were compared with The intraoperative diagnosis which considered to be the standard. They conclude that laser Doppler interferometer was applicable in the clinical sphere and allowed, and has the ability to differentiate many of middle ear pathologies. Many discussions for issues involved in designing time-averaged speckle pattern interferometry system are presented. This leads to measure the guinea pig tympanic membrane vibration response at frequencies up to 4 kHz. The established system was able to measure the nanometer displacements of the TM when stimulated by sound of 70 dB SPL and to obtain phase information on the TM vibration. The results showed that the displacement amplitude increases linearly when the sound pressure level increases [7]. The mechanics of the rat middle ear was investigated by using laser Doppler vibrometer to measure the frequency responses at multiple points on the tympanic membrane and manubrium. Tympanic-membrane vibrations were presented for seven different points in the frequency range of 1 to 10 kHz. The linearity of the rat tympanic membrane for sound-pressure levels between 23 and 59 dB SPL was observed [8]. Then, the practical results of using laser Dopplervibrometer was presented in live human for diagnosis and differentiation of ossicular disorders in patients with aerated middle ears and intact tympanic membranes [9]. Also, the Laser Doppler Vibrometry measurement was used as intraoperative assessment of ossicular chain reconstruction. Results showed that the Laser Doppler Vibrometry can be considered as a valuable noncontactintraoperative tool for measurements of the middle ear response [10]. The pneumatic response of the tympanic membrane was studied to evaluate middle ear pressure by using a pneumatic to scope integrated with low coherence interferometry that was adapted with a pressure-generating system. The displacement of the tympanic membrane was measured under pneumatic pressure transients. They conclude that the presence of a middle ear effusion decreased the pneumatic TM mobility and the middle ear pressure [11]. Later, the high-resolution imaging for the vibration of a rubber membrane within an ear model was provided. In which, a compact optical interferometry was used by transmitting harmonic sound waves stimulations through the otoscope insufflation port and then they analyzed the spectral interferograms [12].

4. Contribution

Previous studies referred to the robustness of interferograms to obtain desired solutions with high precision, therefore Michelson interferometer handled to establish an accurate eardrum vibrations measurement simulation. The contribution in this work is the modification of Michelson interferometer to integrate the behavior of human eardrum. The simulated eardrum vibrations measurement requires adapting the boundary conditions, which is inspired from the real biological eardrum of human. The adaptation includes set the tilt opacity of the middle mirror in the Michelson interferometer, and the best choosing of the material that identify the optical characteristics of the typical eardrum.

5. Design and Implementation

Michelson interferometer was modeled using Zemax OpticsStudio for eardrum design and simulation. Zemax OpticsStudio is comprehensive optical design software that is used to design and analyze optical systems, it deals with ray tracing, modeling the propagation of rays through an optical system. This is carried out by modeling the effect of optical elements such as lenses, mirrors, and diffractive optical elements, for producing standard analysis diagrams [13].

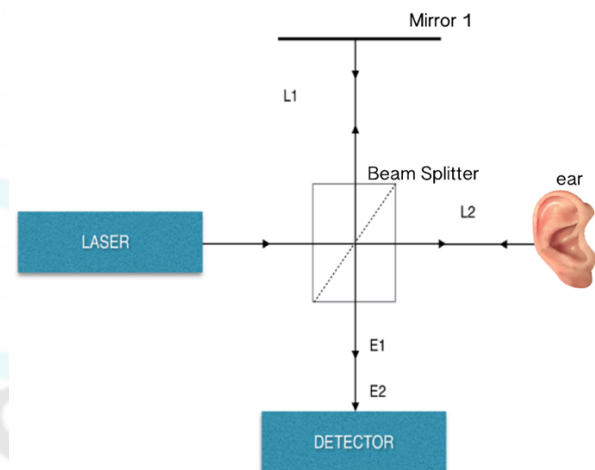


Figure 3: Proposed simulated eardrum of human based on Michelson

The procedure of designing the proposed interferometer deals with the template empty window appeared in the main interface of the Zemax OpticsStudio software. The main interface contains (File, Editors, Analysis, Tools, Reports, Macro, Extensions, Window and Help) options in the taskbar each of which has its specific features that helps for the design process. Non-sequential mode was implemented to model Michelson interferometer in order to trace multiple ray paths at once, this is due to the non-sequential ray tracing allows rays to strike surfaces in any number of times with automatic ray splitting where rays will interact with system components in away similar to that in reality. The Non-Sequential Component Editor, (NSCE) will appear as shown in Fig. 4. From Settings dialog for layouts and raytrace, Split Rays must be checked in order to follow all transmitted and reflected paths as shown in Fig. 5 and Fig. 6.

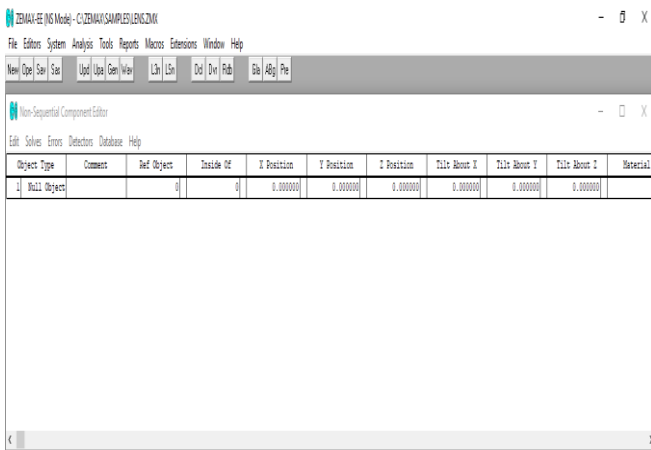


Figure 4: Non-Sequential Component Editor interferometer

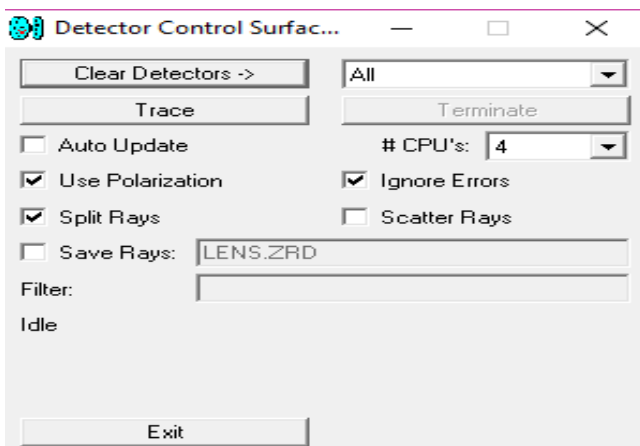


Figure 5: Detector control setting

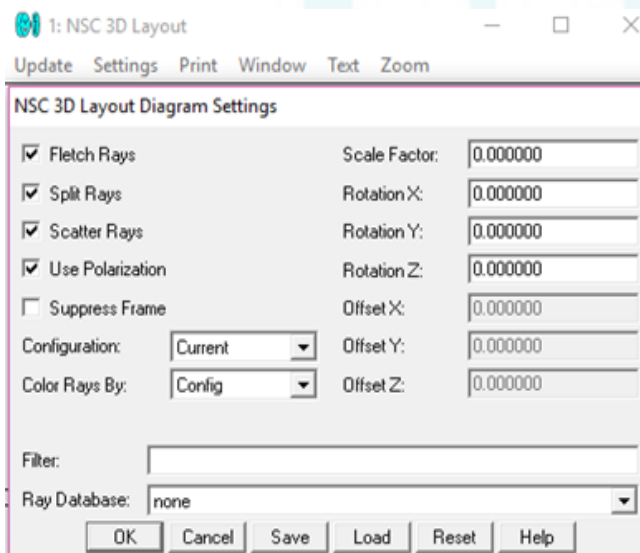


Figure 6 Layout diagram settings

The optical system consists of input beam, beam splitter, mirrors, and detector. The initial parameters such as wavelengths, dimensions, are inserted into the software. The light source chosen used for the interferometer is a diode

laser with a wavelength of 650 nm. In the design the source ellipse used with the wavelength defined in the system explorer as shown in Fig. 7.

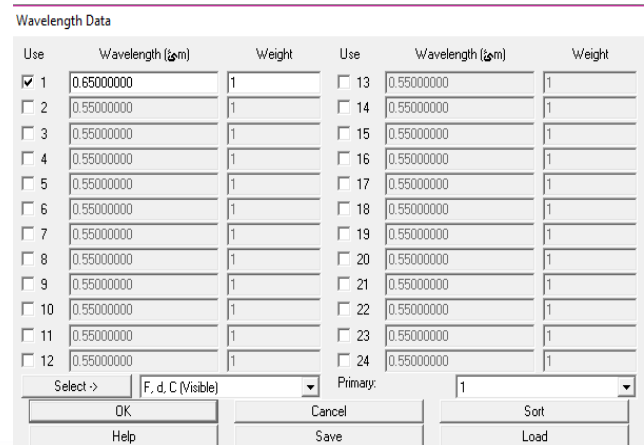


Figure 7: Wavelength data setting

The source parameters used in the editor were: Z position, Layout rays, and Analysis rays that set to be equal to 45, 5, and 75000 frequently. The beam splitter is composed of two rectangular volume, object 3 reference object was taken as -1 in order to make the two rectangular objects acts as a single object within the design.

In the real clinical test, the human eardrum is the moving object whom displacement needed to be detect.in our design the human ear was represented as an ellipse object with a material of Mirror. Since the human ear canal length is 25 mm in average, the length of the test arm of the interferometer in the design was determined to be :

$$\text{Test arm length} = 25 + x$$

where x is integer refers to the number of trial times till reaching the minimal dimensions that achieves best resolution.

The reference arm is an ellipse object with a material of mirror. Finally, the detector object that named as Detector Rect was used in order to analyze the irradiance distribution of the resulted interference beam when its five parameters: X Half width, Y Half width, #X Pixels, #Y Pixels, and Absorb frequently. Therefore, the final system settings in the non-sequential component editor are shown in Fig. 8. While, figure 9 shows the optical layout of Michelson interferometer. The optical system can be visualized through NSC 3D layout window which shows non sequential rays traced from the source object surface to the detector surface. The NSC Shaded Model Layout of Michelson interferometer shows the results of analysis ray traces in Fig. 10.

| Object Type | Comment | Ref Object | Inside Of | X Position | Y Position | Z Position | Tilt About X | Tilt About Y | Tilt About Z | Material |
|------------------|---------|------------|-----------|------------|------------|------------|--------------|--------------|--------------|----------|
| 1 Source Ellip. | Laser | 0 | 0 | 0.000000 | 0.000000 | 65.000000 | 0.000000 | 0.000000 | 0.000000 | |
| 2 Wall Object | | 0 | 0 | 0.000000 | 0.000000 | 0.000000 | 0.000000 | 0.000000 | 0.000000 | |
| 3 Rectangular... | Lc | 0 | 0 | 0.000000 | 0.000000 | 60.000000 | 180.000000 | 0.000000 | 0.000000 | |
| 4 Rectangular... | Lc | -1 | 0 | 0.000000 | 0.000000 | 0.000000 | 180.000000 | 0.000000 | 0.000000 | |
| 5 Wall Object | | 0 | 0 | 0.000000 | 0.000000 | 0.000000 | 0.000000 | 0.000000 | 0.000000 | |
| 6 Ellipse | | 0 | 0 | 0.000000 | 0.000000 | 115.000000 | 0.000000 | 0.000000 | 0.000000 | MI |
| 7 Ellipse | | 0 | 0 | 0.000000 | 55.000000 | 60.000000 | 90.000000 | 0.000000 | 0.000000 | MI |
| 8 Wall Object | | 0 | 0 | 0.000000 | 0.000000 | 0.000000 | 0.000000 | 0.000000 | 0.000000 | |
| 9 Detector Rect | | 0 | 0 | 0.000000 | -10.000000 | 60.000000 | 90.000000 | 0.000000 | 0.000000 | AS |

Figure 8: Final design settings

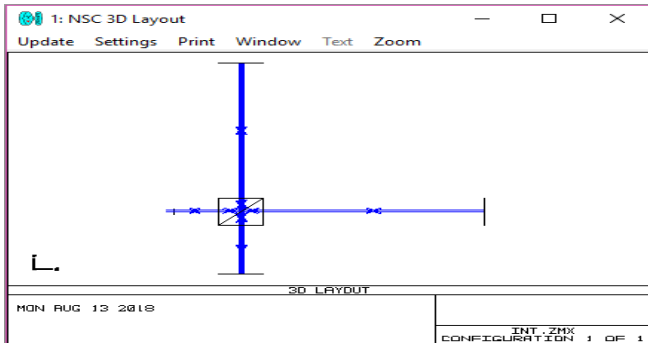


Figure 9: 3D Layout and Model

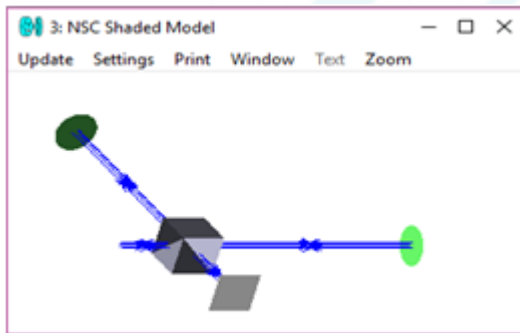


Figure 10: NSC shaded model layout

In order to decrease the size of the device, a pentaprism was introduced in the interferometer design for shortening the optical path length since it can deviate the incident beam in the reference arm of interferometer without inverting or reversing to 90°. The size of the pentaprism should be about 10 mm. The variant scaled system settings in the non-sequential component editor are shown in Fig. 11.

| Object Type | Comment | Ref Object | Inside Of | X Position | Y Position | Z Position | Tilt About X | Tilt About Y | Tilt About Z | Material |
|------------------|-----------|------------|-----------|------------|------------|------------|---------------|--------------|--------------|----------|
| 1 Source Ellip. | Laser | 0 | 0 | 0.000000 | 0.000000 | 65.000000 | 0.000000 | 0.000000 | 0.000000 | |
| 2 Wall Object | | 0 | 0 | 0.000000 | 0.000000 | 0.000000 | 0.000000 | 0.000000 | 0.000000 | |
| 3 Rectangular... | Lc | 0 | 0 | 0.000000 | 0.000000 | 60.000000 | 180.000000 | 0.000000 | 0.000000 | |
| 4 Rectangular... | Lc | -1 | 0 | 0.000000 | 0.000000 | 0.000000 | 180.000000 | 0.000000 | 0.000000 | |
| 5 Wall Object | | 0 | 0 | 0.000000 | 0.000000 | 0.000000 | 0.000000 | 0.000000 | 0.000000 | |
| 6 Poly Object | pentapris | 0 | 0 | 0.000000 | 15.000000 | 60.000000 | -90.000000 | 0.000000 | 0.000000 | |
| 7 Wall Object | | 0 | 0 | 0.000000 | 0.000000 | 0.000000 | 0.000000 | 0.000000 | 0.000000 | |
| 8 Ellipse | | 0 | 0 | 0.000000 | 0.000000 | 115.000000 | 1.000000E-100 | 0.000000 | 0.000000 | MI |
| 9 Ellipse | | 0 | 0 | 0.000000 | 20.000000 | 70.000000 | 0.000000 | 0.000000 | 0.000000 | MI |
| 10 Standard Lens | Ld2560 | 0 | 0 | 0.000000 | -1.000000 | 60.000000 | 90.000000 | 0.000000 | 0.000000 | SI |
| 11 Wall Object | | 0 | 0 | 0.000000 | 0.000000 | 0.000000 | 0.000000 | 0.000000 | 0.000000 | |
| 12 Detector Rect | | 0 | 0 | 0.000000 | -10.000000 | 60.000000 | 90.000000 | 0.000000 | 0.000000 | AS |

Figure 11: The variant scaled system design setting

Figures 12 and 13 show 3D Layout and NSC shaded model of the interferometer design when pentaprism introduced in the reference arm. The laser beam from a beam splitter is deflected perpendicularly by the pentaprism, reflected from the reference mirror and deflected again by the pentaprism towards the beam splitter. In order to limit the ray paths when viewing the results in the Layout Plot, Filter strings was used. The rays which originate from source and reach the detector are important for analysis results. So we applied the Hn filter to Detector Object 12 as shown in Fig. 14 and

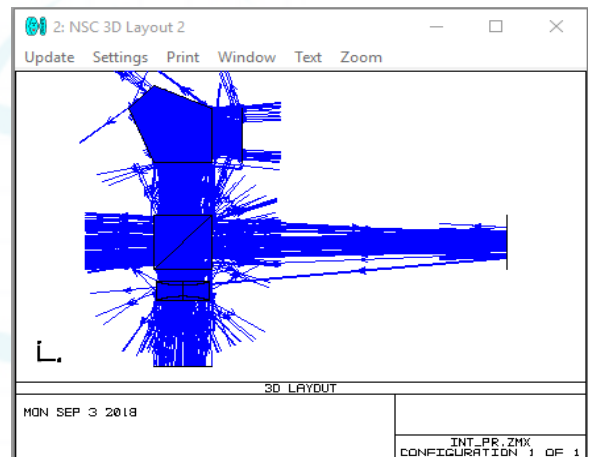


Figure 12: Layout of the variant scaled interferometer

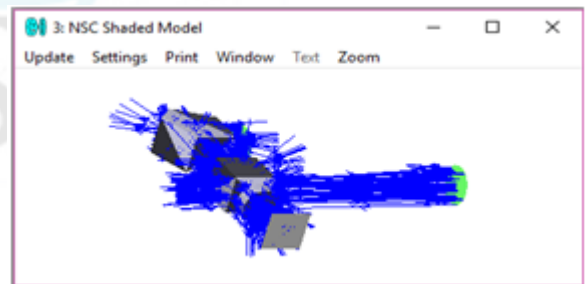


Figure 13 NSC shaded model of the variant scaled interferometer

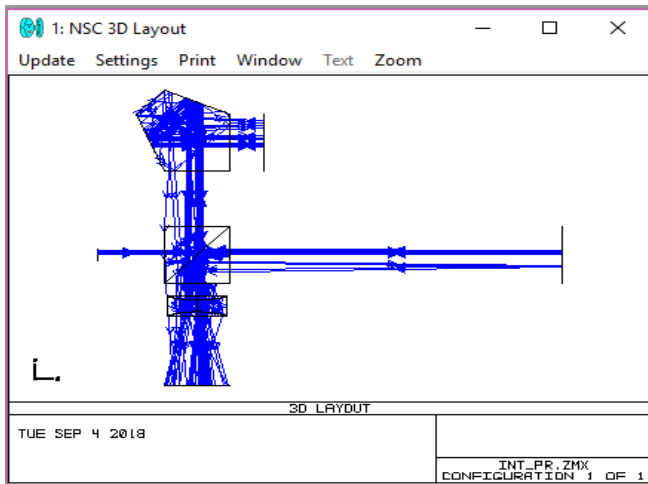


Figure 14: 3D Layout of interferometer after applying Hn filter

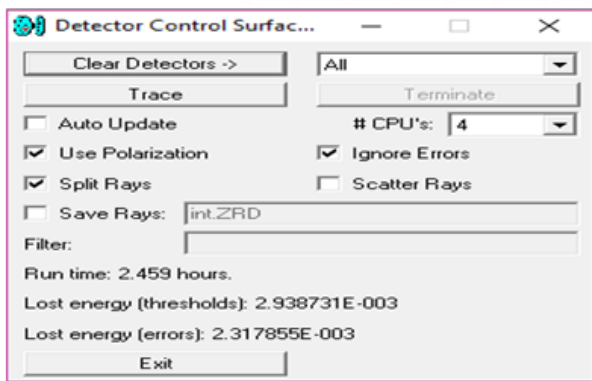


Figure 15: Detector control window

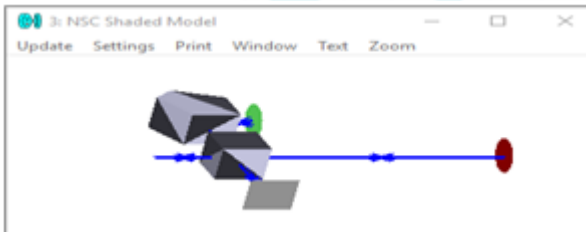


Figure 16: Detector image of the interferometer

6. Simulation Results

To analyze the simulation results, the irradiance distribution is displayed on the Detector viewer by clicking on Dct button on the Zemax button bar. Because rays may split at interfaces, the polarization information are needed for precise reflection and transmission computation. Also, in order to see ray splitting in the properties of 3D Layout, "Split Rays" and "Use Polarization" are both checked in the detector control window. The detector must be cleared from any data of previous trace by clicking on clear detectors then "trace" button to start a ray trace and finally "Exit" when Zemax completed ray tracing as shown in Fig. 15.

The degree of interference between the two interferometer's paths can be analyzed by using the Coherent Irradiance option of the detector viewer. In this setting the energy of each ray reaching the detector will be added coherently according to its amplitude and phase. Figures 16 and 17 show the detector image of resolution 200 pixels per 10 mm that

contains a bright central spot without surrounding rings, this is because the light waves were in phase due to the arms of the interferometer have equal path length ($d_1=d_2$). The number of total hits is consistent with 750,000 source rays being doubled by the splitting and successive scattering surfaces. The highest the total hits are preferred to produce a high-contrast fringe pattern. In order to obtain an interference pattern, a small optical path difference will be introduced by tilting the reference mirror, the interference pattern was shown as given in Fig. 18.

Stripe interference pattern appears on the image plane results from optical path difference between the interferometer arms due to the tilt of the reference mirror. Figure 19 shows the detector image of 200 pixels per 10 mm resolution with interference stripes. For a plane mirror, the interference pattern will appear as stripes not fringes. Total power has gone up to 6.292 W. The maximum power on one pixel of the detector (Peak Irradiance) increases in turn to 9.57 W/cm^2 .

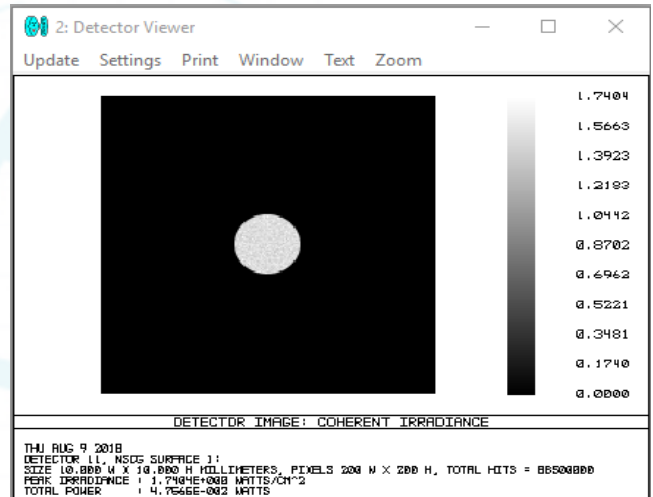


Figure 17: Detector image of the scaled interferometer

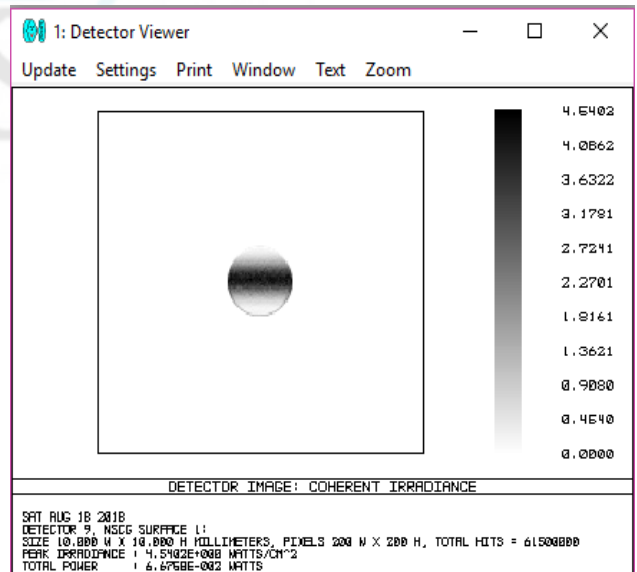


Figure 18: Interference pattern

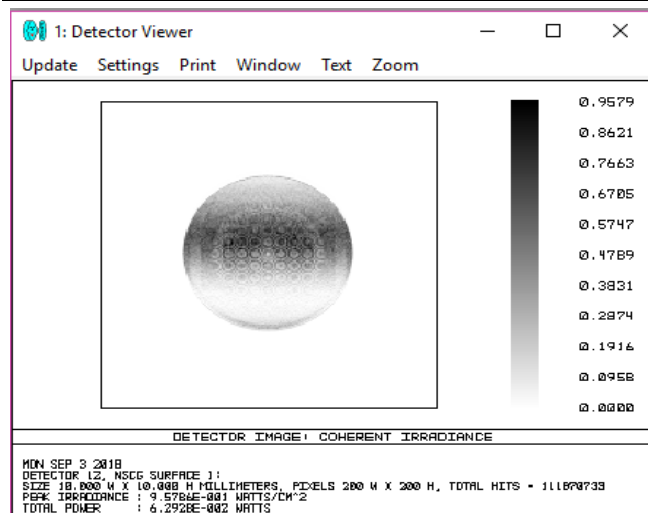


Figure 19: Interference pattern of the scaled interferometer

7. Conclusions

Default Michelson interferometer design was proposed and simulated by ZemaxOpticStudio, then a variant design was used to reduce the interferometer dimensions and improve its performance. The results in detector viewer of the second design showed that the peak irradiance increased when the distance travelled by the light beam decreased. This leads to increase the power and improve the interferometer's resolution

Portable Michelson interferometer device for eardrum evaluation was implemented with the optical distances determined from Zemax OpticStudio simulation results. This device was used to evaluate the eardrum characteristics in response to pure tone sound stimulations. The measurement results show that the device was able to detect nanometer displacement of the tympanic membrane with a high sensitivity.

References

- [1] A. A. Freschi, N. R. Caetano, G. A. Santarine, and R. Hessel, "Laser interferometric characterization of a vibrating speaker system," *Am. J. Phys.*, vol. 71, no. 11, pp. 1121–1126, 2003.
- [2] R. Bommarreddi, "Applications of Optical Interferometer Techniques for Precision Measurements of Changes in Temperature, Growth and Refractive Index of Materials," *Technologies*, vol. 2, no. 2, pp. 54–75, 2014.
- [3] D. D. Nolte, *Optical Interferometry for Biology and Medicine*. New York, NY: Springer New York, 2012.
- [4] R. Z. Gan, "Diagnosis and Characterization of Middle-ear and Cochlear Functions," pp. 95–112, 2013.
- [5] H. M. Kjer and R. R. Paulsen, "Modelling of the Human Inner Ear Anatomy and Variability for Cochlear Implant Applications," 2015.
- [6] A. Huber, M. Ferrazzini, and U. Willi, "[Laser doppler interferometry, a new clinical instrument?].," *Schweiz. Med. Wochenschr.*, vol. Suppl 125, p. 80S–82S, 2000.
- [7] H. Wada *et al.*, "Vibration measurement of the tympanic membrane of guinea pig temporal bones using

time-averaged speckle pattern interferometry," *J. Acoust. Soc. Am.*, vol. 111, no. 5, p. 2189, 2002.

- [8] F. Akache and W. R. J. S. J. Daniel, "An Experimental Study of Tympanic Membrane and Manubrium Vibrations in Rats Keywords Comparative Anatomy Comparative Anatomy Specimen Preparation," no. 514, 2007.
- [9] A. Manuscript and P. H. Ears, "NIH Public Access," *October*, vol. 29, no. 1, pp. 3–19, 2008.
- [10] J. Sokołowski, M. Lachowska, R. Bartoszewicz, and K. Niemczyk, "Methodology for Intraoperative Laser Doppler Vibrometry Measurements of Ossicular Chain Reconstruction.," *Clin. Exp. Otorhinolaryngol.*, vol. 9, no. 2, pp. 98–103, Jun. 2016.
- [11] J. Won *et al.*, "Pneumatic low-coherence interferometry otoscope to quantify tympanic membrane mobility and middle ear pressure," *Biomed. Opt. Express*, vol. 9, no. 2, p. 397, Feb. 2018.
- [12] S. Grechin and D. Yelin, "Imaging acoustic vibrations in an ear model using spectrally encoded interferometry," *Opt. Commun.*, vol. 407, pp. 175–180, Jan. 2018.
- [13] "q 2006 by Taylor & Francis Group, LLC," 2006.

Author Profile



Suha M. Khorsheed, received the B.S., M.S., and Ph.D. degrees in Physics from Al-Nahrain University in 1995, 2000, and 2007, respectively. During 2007–2016, she stayed in Advanced Photonics Laboratory to modify and improve performance of optical systems. She now lecturer in the Physics Department- College of Science in Al-Nahrain University.

Raya Badie Younis, Received the B.Sc. degree in Biomedical Engineering from Al-Nahrain university /College of engineering, Iraq. Now M.Sc. student at Biomedical Eng. Dept./ College of Eng. Al-Nahrain University, Baghdad-Iraq.



Ziad Tarik Al-Dahan, received the P.G. Diploma (1985), M.Phil. (1986) and Ph.D. (1988) from Brunel University, UK. Now Professor at Biomedical Eng. Dept./ College of Eng. Al-Nahrain University, Baghdad-Iraq.